Journal of Alzheimers Disease & Parkinsonism

Yamashima, et al. J Alzheimers Dis Parkinsonism 2022, 12:1
ISSN: 2161-0460

Research Article Open Access

Hydroxynonenal Causes Lysosomal and Autophagic Failure in the Monkey POMC Neurons

Tetsumori Yamashima[1,2],* Piyakarn Boontem[2,3], Hidenori Kido[4] Masahiro Yanagi[4], Takuya Seike[4], Daisuke Yamamiya[4], Shihui Li[4], Tatsuya Yamashita[2,4], Mitsuru Kikuchi[1] and Eishiro Mizukoshi[4]

[1]*Department of Psychiatry and Behavioral Science, Kanazawa University Graduate School of Medical Sciences, Kanazawa, Japan*
[2]*Department of Cell Metabolism and Nutrition, Kanazawa University Graduate School of Medical Sciences, Kanazawa, Japan*
[3]*Division of Anatomy, University of Phayao, Mae Ka, Thailand*
[4]*Department of Gastroenterology, Kanazawa University Graduate School of Medical Sciences, Kanazawa, Japan*

Abstract

Nowadays, overweight people have increased worldwide, giving rise to global 'obesity epidemic'. Appetite and energy balance are regulated by the arcuate nucleus of hypothalamus. Pro-opiomelanocortin (POMC) neurons play an important role for the appetite suppression by sensing leptin, insulin, free fatty acids, etc. in the blood. High-fat diet is known to be associated with POMC neurodegeneration and related lifestyle-related diseases by generating reactive oxygen species. However, the mechanism by which excessive fatty acids induce POMC neurodegeneration remains unknown. We recently reported that lipid-peroxidation product 'hydroxynonenal' causes lysosomal membrane disintegrity *via* calpain-mediated cleavage of the oxidized (carbonylated) Hsp70.1. After the consecutive injections of synthetic hydroxynonenal in monkeys to make the serum concentration relevant to human 60's, here we studied its adverse effect upon POMC neurons. By light microscopy, many POMC neurons showed dissolution of the cytoplasm and nuclear chromatin, and were positive for Fluoro-Jade C staining. Immunoreactivities of GPR40 (free fatty acid receptor), μ-calpain (Ca^{2+}-dependent papain-like protease), Hsp70.1 (chaperone protein and lysosomal stabilizer), and p62 (chaperone for autophagic removal), showed an increased immunoreactivity within the degenerating POMC neurons. Albeit the decrease of POMC neurons in the arcuate nucleus tissue, Western blotting could confirm slight upregulation of these proteins. Furthermore, permeabilization of the lysosomal limiting membrane was suggested by the enlarged immunoreactive area double-positive for Lamp-2 and cathepsin B. Electron-microscopic analysis showed a remarkable decrease of lysosomes and a concomitant increase of autophagosomes. Lysosomes measuring 300~500 nm were round or oval with the distinct limiting membrane, whereas autophagosomes measuring 350~800 nm had an irregular configuration, being devoid of the limiting membrane. Lysosomes prior to fusing with autophagosomes showed permeabilization of the limiting membrane. Although up-regulation of the calpain-mediated Hsp70.1 cleavage was hardly demonstrated on immunoblots because of the POMC neuronal loss, Hsp70.1 disorder presumably contributed to the lysosomal membrane disintegrity and autophagy deficiency.

Keywords: Arcuate nucleus; GPR40; Hsp70.1; Hypothalamus; Obesity

Abbreviations: AgRP: Agouti-related Peptide; BMP: Bis(monoacylglycero) Phosphate; CA-1: *Cornu Ammonis* 1; DAPI: 4', 6-diamidino-2-phenylindole; GPR40: G protein-coupled receptor 40; Hsp70.1: Heat-shock Protein70.1; HNE: hydroxynonenal; Lamp-2: lysosomal associated Membrane Protein 2; LMP: Lysosomal Membrane Permeabilization; NPY: Neuropeptide; POMC: Pro-Opiomelanocortin; PUFA: Polyunsaturated Fatty Acids; ROS: Reactive Oxygen Species

Introduction

A major shift in our nutritional environment in recent years has contributed to 'obesity epidemic'. According to the World Health Organization, more than 1.9 billion adults and 42 million children under the age of 5 are currently overweight. Obesity has long been considered the result of a lack of discipline and effort to reduce calorie intake and to increase physical activity. However, extensive research in humans, monkeys, and rodents recently revealed that a complex interplay of genes, food habits, and environmental factors impact the hypothalamic control of energy homeostasis and body weight control [1,2]. Hypothalamus is a critical region for regulating appetite, body weight, and energy homeostasis. Due to its anatomical localization, hypothalamus can sense and integrate metabolic information from the periphery, and dictate neural output commands to the corresponding organs. In particular, the arcuate nucleus of hypothalamus is related to the control of feeding behavior. It is located close to the median eminence at the ventromedial part of hypothalamus, which is rich in fenestrated capillaries to form a leaky blood-brain barrier. So, this facilitates transport of peripheral hormonal and nutrient signals and their sensing by the arcuate nucleus neurons [3].

There are two neuronal populations in the arcuate nucleus: pro-opiomelanocortin (POMC)-expressing neurons and neuropeptide Y/agouti-related peptide (NPY/AgRP)-expressing neurons. POMC and NPY/AgRP neurons are in a good position to integrate peripheral (nutrients and hormones) and central (neuropeptides and neurotransmitters) inputs to produce a central command for feeding behavior. For instance, the anorexigenic (appetite-suppressing) effects of leptin and serotonin are mediated by excitation of POMC neurons and suppression of NPY/AgRP neurons [4-7]. On the contrary, the orexigenic (appetite-stimulating) effect of ghrelin suppresses POMC neurons but excites NPY/AgRP neurons [8-10]. The POMC neuronal activation reduces food intake and increases energy expenditure, whereas the NPY/AgRP neuronal activation induces food intake and decreases energy expenditure [11-15]. Other than leptin and serotonin, POMC neurons respond to diverse circulating signals such

***Corresponding author:** Dr. Tetsumori Yamashima, Departments of Psychiatry and Behavioral Science and Cell Metabolism and Nutrition, Kanazawa University Graduate School of Medical Sciences, Takara-Machi 13-1, Kanazawa, 920-8041 Japan, Tel: +81) 90 2129-1429; E-mail: yamashima215@gmail.com

Received: 17-Jan-2021, Manuscript No. JADP-21-55307; **Editor assigned:** 19-Jan-2022, PreQC No. JADP-21-55307 (PQ); **Reviewed:** 3-Feb-2022, QC No. JADP-21-55307; **Revised:** 7-Feb-2022, Manuscript No. JADP-21-55307 (R); **Published:** 14-Feb-2022, DOI: 10.4172/2161-0460.1000529.

Citation: Yamashima T, Boontem P, Kido H, Yanagi M, Seike T, et al. (2022) Hydroxynonenal Causes Lysosomal and Autophagic Failure in the Monkey POMC Neurons. J Alzheimers Dis Parkinsonism 12: 529.

as glucose, insulin, ghrelin, peptide YY, and most importantly, to long-chain fatty acids [4,16-23] to regulate energy expenditure by releasing melanocyte-stimulating hormones (MSH) such as α-MSH and γ-MSH [24]. The hypothalamic effects of adiposity hormones such as leptin and insulin, and nutrients such as free fatty acids, down-regulate the energy homeostasis by inhibiting food intake and liver glucose production with MSH. Physiological increments in plasma fatty acids are sensed within hypothalamus, which is required to balance their direct stimulatory action on hepatic gluconeogenesis and energy balance [25]. Under the caloric abundance, however, rapid onset of the hypothalamic resistance to leptin, insulin and fatty acids contributes to the susceptibility to obesity and insulin resistance [26]. Importantly, it still remains unelucidated what means the hypothalamic resistance, or what is a causative factor [27-32].

In 2003, two groups independently found G protein-coupled receptor 40 (GPR40) as a receptor for medium-to long-chain fatty acids [33,34]. Briscoe et al. demonstrated that GPR40 mRNA expression is most abundant in the brain among human organs. Thereafter, GPR40 was reported to be crucial for both physiological (adult neurogenesis in the hippocampus and energy control in the hypothalamus) and pathological (stroke, Alzheimer's disease, Parkinson's disease, and type 2 diabetes) conditions [35-38]. GPR40 has dual roles in response to the amount and status of ligands: i.e. an appropriate amount of non-oxidized polyunsaturated fatty acids (PUFA) participates in the physiological function, whereas excessive and/or oxidized PUFA induce abnormal Ca^{2+} mobilization to trigger cell degeneration/death [39]. Unlike NPY/Agrp neurons, POMC neurons are stimulated by input from free (non-esterified) fatty acids in the blood [4,20]. By high-fat diets or deep-fried foods, free fatty acids become excessive in the blood, which are prone to be oxidation. Both excessive PUFA and oxidized PUFA induce abnormal calpain activation by the over activation of GPR40 [40-42]. Consequently, cells with abundant GPR40 receptors develop degeneration/death. For instance, in response to the oxidized PUFA such as conjugated linoleic acid [43] or trans-isomers of arachidonic acid [44,45], GPR40 was demonstrated to mediate lipotoxicity in β-cells, neurons, or microvessels *via* abnormal Ca^{2+} mobilization, which results in diabetes, retinopathy, or stroke, respectively. As POMC neurons show expression of GPR40, they may respond not only to the excessive fatty acids but also to the lipid-peroxidation product, 'hydroxynonenal' [2,39]. This may facilitate inhibiting appetite-suppression and energy expenditure and inducing obesity by POMC neurodegeneration.

Although hypothalamic neurons sense circulating fatty acids in the normal conditions [29], lipid overload due to high-fat diets, especially saturated fatty acids, is known to trigger cell stress in these neurons [46,47]. A considerable amount of evidence shows that reactive oxygen species (ROS) in the mammalian brain are directly responsible for the oxidation of membrane phospholipids. However, the exact causal relation among ROS generation, ω-6 PUFA oxidation, and neuronal degeneration/death, still remains incompletely understood [48-50]. In response to ROS, linoleic and arachidonic acids in the membrane phospholipids are known to generate intrinsic hydroxynonenal. In addition, during deep-frying of the cooking oils containing linoleic acids, exogenous hydroxynonenal is generated. Using the monkey experimental paradigm, Yamashima et al. recently reported that brain neurons, hepatocytes and pancreatic Langerhans cells show similar degeneration/death after the consecutive injections of the synthetic hydroxynonenal. Accordingly, they suggested that independent to the cell type-specific differences, exogenous and/or intrinsic hydroxynonenal may induce diverse cell degeneration/death in humans for the progression of lifestyle-related diseases [2,51,52]. Using the same monkey experimental paradigm, here we found that the synthetic hydroxynonenal causes POMC neuronal degeneration/death by inducing both lysosomal membrane disintegrity and autophagy deficiency. To the best of our knowledge, this may be the first report to implicate hydroxynonenal for POMC neurodegeneration as a possible cause of obesity.

Materials and Methods

Animals

After the referee of animal experimentation about the ethical or animal welfare, young (4~5 years: compatible with teenagers in humans) female Japanese macaque monkeys (Macaca fuscata) were supplied by National Bio-Resource Project (NBRP) "Japanese monkey" (National Institute for Physiological Sciences, Okazaki, Japan). After arrival, at least for 1 year to facilitate acclimation, the monkeys were reared in the wide cage with autofeeding and autodrainage machines as well as appropriate toys to play. The room temperature was kept 22°C ~24°C with the humidity of 40%~50%. They were fed by 35 kCal/Kg body weight of non-purified solid monkey foods per day containing PUFA and vitamins. In addition, apples, pumpkins, sweet potatoes, or nuts were given twice every week. The health and well-being of the animals were monitored by checking the consumption of foods, pupilar reflex to the light, and conditions of standing and jumping. At 5~6 years of age, five healthy monkeys with body weight 5~7 Kg were randomly divided into two groups of the sham-operated control (n=2) and those undergoing hyroxynonenal injections (n=3). In 3 monkeys, under the intramuscular injection of 2 mg/Kg of kethamine hydrochloride, intravenous injections of 5 mg/week of synthetic hydroxynonenal (Cayman Chemical, Michigan, USA) were done for 24 weeks (total doses: 120 mg). Such doses and serial injections were designed to temporarily replicate blood concentrations of hydroxynonenal in humans around 60's [53]. Three monkeys after the hydroxynonenal injections were served for the histological, immunohistochemical, electron-microscopic, and Western blotting analyses, while the remaining two monkeys were served as controls. We were obliged to restrict the number of animals due to the cost of both animals and the synthetic hydroxynonenal.

Tissue collection

Six months after the initial injection and within a couple of weeks after the final injection, the monkeys were immobilized by the intramuscular injection of 10 mg/Kg ketamine hydrochloride followed by the intravenous injection of 50 mg/Kg sodium pentobarbital. Furthermore, to ameliorate animal suffering, the monkey was deeply anesthetized with 1.5% halothane plus 60% nitrous oxide. After 500 mL of saline was perfused through the left ventricle, the brain was resected to excise the arcuate nucleus in the hypothalamus.

Histological and immunofluorescence histochemical analyses

The arcuate nucleus tissue after fixation with 4% paraformaldehyde for 2 weeks was embedded in paraffin, and 5 μm sections were stained by hematoxylin and eosin (H-E). For the immunofluorescence histochemistry, the cryoprotected tissues embedded in the OCT medium (Sakura Finetek, Japan) were cut by cryotome (Tissue-Tek®Polar®, Sakura, Japan), and 5 μm sections were soaked with heated 0.01% Citrate retrieval buffer to enhance epitope retrieval. Non-specific staining was blocked with 1% bovine serum albumin (Nacalai tesque, Japan), and were incubated overnight at 4°C with the primary antibodies at the dilution of 1:100. We used mouse monoclonal anti-human Hsp70 (BD Bioscience, USA), rabbit anti-human activated μ-calpain (order made by PEPTIDE Institute, Japan), rabbit anti-human cathepsin B (Cell Signaling, USA), mouse monoclonal anti-lysosome-

associated membrane protein 2 (Lamp-2)(Invitrogen, USA), rabbit anti-human p62 (Abcam, USA), rabbit anti-human POMC (Abcam, USA) and mouse anti-human POMC (LSBio, USA) antibodies. After washings with 0.1% PBST, the sections were incubated in dark room for 30 min with secondary antibodies; Alexa Fluor™ 594 goat anti-mouse IgG [H+L] (Invitrogen, USA), or Alexa Fluor™ 488 goat anti-rabbit IgG (Invitrogen, USA) at the dilution of 1:500. To block autofluorescent staining, Autofluorescence Quenching Kit (Vector Laboratories, USA) was utilized. The immunoreactivity was observed with the laser scanning confocal microscope (LSM5 PASCAL, Software ZEN 2009, Carls Zeiss, Germany).

Electron microscopic analysis

Small specimens of each tissue were fixed in 2.5% glutaraldehyde for 2h and 1% OsO4 for 1h. Subsequently, they were dehydrated with graded acetone, embedded in resin (Quetol 812, Nisshin EM Co. Tokyo), and thin sections were made. After trimming with 0.5% toluidine blue-stained sections, the ultrathin (70 nm) sections of appropriate portions were stained with uranyl acetate (15 min) and lead citrate (3 min), and were observed by the electron microscope (JEM-1400 Plus, JEOL Ltd., Tokyo).

Western blotting

Arcuate nucleus tissues were homogenized in RIPA buffer containing lysis buffer (Millipore, USA), protease inhibitor cocktail (Roche, Germany) on ice. The homogenized samples were centrifuged at 12,000 rpm, 4°C for 10 min, the supernatant protein concentrations were determined by utilizing the BCA protein kit (Thermo Fisher, USA). Twenty µg proteins were separated by SDS-PAGE on 5%-20% gel (SuperSep™ Ace gel, Wako, Japan) at 40 mA for 1h. The total proteins were transferred to PVDF membrane (Millipore, USA). Transferred protein quality was checked with Ponceau S solution (Sigma-Aldrich, USA). Then, the transferred proteins were blocked with 0.2% blocking solution (KPL Detector™ Block, USA) for 1h. The blots were incubated with mouse monoclonal anti-human Hsp70 antibody (BD Bioscience, USA) at the dilution of 1:4,000, rabbit anti-human activated µ-calpain antibody (PEPTIDE Institute, Japan) at 1:250, anti-p62 (Abcam, USA) at 1: 1000, anti-Lamp-2 antibody (Invitrogen, USA) at 1:500, and rabbit anti-human GPR40 antibody (LSBio, USA) at 1:500 overnight on shaker. β-actin was utilized as an internal control at a dilution of 1:10,000 (Sigma-Aldrich, USA). The immunoblots were subsequently incubated for 1h with secondary antibodies at 1:10,000 dilution of anti-mouse (Santa Cruz, USA) or anti-rabbit IgG (Sigma, USA). The enhanced chemiluminescent signals were visualized using HRP substrate detection kit (Millipore, USA) and ImageQuant LAS 4000 imaging system (GE Life Science, USA).

Fluoro-Jade C staining

Fluoro-Jade C (Fluoro-Jade® C RTD™ Staining Reagent Kit, Biosensis, Australia) was used to label the degenerating neurons as reported previously [25]. Thirty µm-thick free-floating sections were soaked in 80% ethanol mixed with solution A (Fluoro-Jade® C RTD™ stain reagent, Biosensis, Australia). The fluorescent background was blocked by solution B (Fluoro-Jade® C RTD™ stain reagent, Biosensis, Australia). FJC staining was done by solution C (Fluoro-Jade® C RTD™ stain reagent, Biosensis, Australia) and nuclear counter stain was done by 4',6-diamidino-2-phenylindole (DAPI) at 1:500 dilution (Nacalai tesque, Japan). The tissues were dried and warmed at 50°C on slide warmer. The FJC staining was observed by laser scanning confocal microscopic system (LSM5 PASCAL, Software ZEN 2009, Carls Zeiss, Germany).

Image acquisition

All immunohistochemistry images were acquired using laser scanning confocal microscope with 40 × and 63 × objective lens and exported in tif file format (LSM5 PASCAL, Software ZEN 2009, Carls Zeiss, Germany). Then image processing and intensity analysis were performed by image fiji software (https://fiji.sc/).

Statistical analysis

The density of protein bands was quantified and normalized by β-actin utilizing FusionCapt Advance analyzing software (Fusion Fx, Vilber Lourmat, France). Five interested areas with POMC neurons were quantified by image fiji software. (https://fiji.sc/). Statistical analysis was done by using GraphPad Prism software 9.2.0 version. All data were showed as mean ± SEM. Student's *t*-test was utilized and $p<0.05$ was considered statistically significant.

Ethics

This study was carried out in strict accordance with the recommendations in the Guide for the Care and Use of Laboratory Animals of the National Institutes of Health. The protocol was approved by the Committee on the Ethics of Animal Experiments of the Kanazawa University Graduate School of Medical Sciences (Protocol Number: AP-153613).

Results

Studying adverse effects of high-fat diets upon the hypothalamic arcuate nucleus of rodents, Thaler et al. found in POMC neurons both accumulation of autophagosomes engulfing damaged mitochondria and an increased immunoreactivity of Hsp72. Interestingly, similar neurodegeneration associated with accumulation of autophagosomes and overexpression of Hsp70.1 (also called Hsp70 or Hsp72), were observed in this study in all 3 monkeys after the consecutive hydroxynonenal injections. Many arcuate nucleus neurons showed degeneration/death which was characterized by dissolution and shrinkage of the cytoplasm on (H-E) staining (Figure 1a, dot circles). Microvacuoles were often seen within and around the soma of degenerating neurons (Figure 1a, open arrows). The FJC staining was negligible in the control neurons, but after hydroxynonenal injections, arcuate nucleus showed numerous FJC-positive neurons (Figure 1b). In addition, by the immunohistochemical analysis, POMC-positive neurons were significantly ($p=0.036$) decreased, compared to the control (Figure 1c). Concomitantly, a remarkable decrease of DPAI-positive nuclei (Figure 1d) was seen, compared to the control. As neither apoptotic bodies nor membrane blebbing were observed, the cell death pattern was thought to be not apoptosis.

As an autophagy receptor, p62 (also known as SQSTM1) assembles misfolded and damaged proteins into aggregates for bulk degradation through the autophagy-lysosome pathway [54,55]. Autophagy substrates are targeted for degradation by associating with p62, a multidomain protein that interacts with the autophagy machinery. Given its role as a chaperone for the autophagic removal of protein and organella cargo, increases of p62 have been used as a marker of autophagy deficiency [56]. In this study, immunohistochemical analysis using anti-p62 antibody showed negligible staining in the arcuate nucleus neurons of control monkeys (Figure 1d upper). In contrast, neurons surviving from hydroxynonenal injections (Figure 1a circles) showed an increased immunoreactivity of p62 as punctuate or coarse-granular pattern (Figure 1d lower).

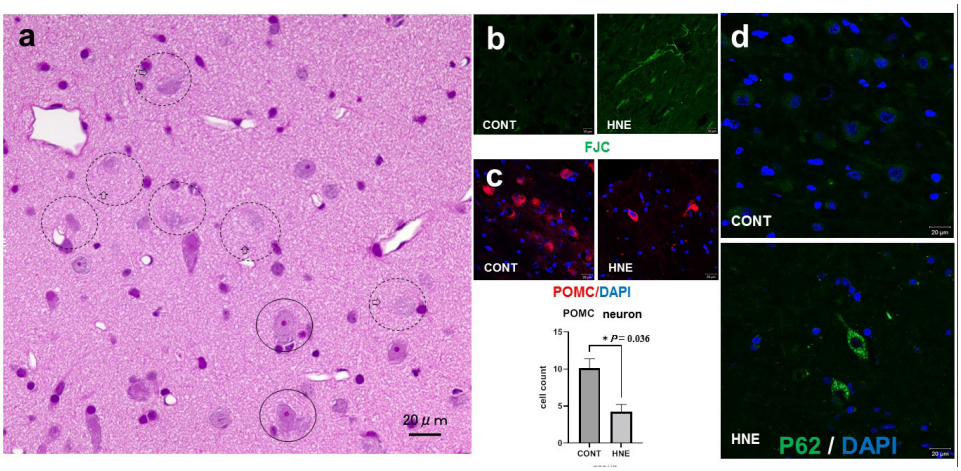

Figure 1: Neuronal degeneration death in the arcuate nucleus of the monkey after the consecutive injections of hydroxynonenal. a: Most of the arcuate nucleus neurons show dissolution of the nuclear chromatin and shrinkage of the cytoplasm (dot circles) with forming pericellular microcysts (open arrows). These almost dead neurons show loss of the nucleolus, while the degenerating, but still alive, neurons show well-preserved nucleolus and nuclear chromatin (circles). The following electron-microscopic analyses (Figures 2,3 and 6) were done mainly in these degenerating neurons, (H-E staining). b: Fluoro-Jade C (FJC) staining was negligible in the control neurons, but the arcuate nucleus after hydroxynonenal injections showed an increase of FJC-positive neurons. c: Immunofluorescence histochemistry shows a significant decrease (lower, p=0.036) of POMC neurons after hydroxynonenal injections (right), compared to the control (left) d: Immunofluorescence histochemistry shows an increase of p62 immunoreactivity in the surviving neurons after hydroxynonenal injections (lower), compared to the control (upper). DAPI staining (blue) shows a significant decrease of cell nuclei.

By the electron-microscopic analysis, the surviving neurons after hydroxynonenal injections showed shrinkage of the cytoplasm with the pericellular microcystic formation (Figure 2b), which was compatible with the H-E finding (Figure 1a open arrows). These microcysts were ultrastructurally identified to be enlarged dendritic processes (Figure 2b) (Figures 3b and 3c). In the control neurons, a large number of lysosomes were seen in the perinuclear cytoplasm (Figure 2a). Most of them were round or oval, measuring 300~500 nm in diameter, and were bound by the distinct limiting membrane (Figure 3a arrows). In contrast, after hydroxynonenal injections, normal lysosomes as seen in the control neurons were remarkably decreased (Figure 2b). Instead, autophagosomes measuring 350~800 nm, being larger than lysosomes (Figure 2a), were increased (Figures 2b and 3b lower rectangle). This was very similar to the hippocampal CA-1 neurons which showed much stronger degeneration with a remarkable increase of autophagosomes (Figure 2b rectangle) [52]. Lysosomes and autophagosomes showed distinct ultrastructural features in size, shape, configuration, and presence of the limiting membrane. It is likely that an increment of autophagosomes was compatible with the overexpression of p62 staining (Figure 1d). Dendritic processes of the POMC-positive neuron showed a marked dissolution of synaptic vesicles, and electron-dense lamellar deposits were seen (Figures 3b upper rectangle and 3c), both of which were not seen in the control neurons.

During normal autophagy, autophagosomes containing aged/damaged intracellular components and/or organelle bind with lysosomes to form autolysosomes (or autophagolysosomes), in which the sequestered contents are degraded by lysosomal cathepsin enzymes for recycling. However, in the cells undergoing severe oxidative stress, autophagy deficiency, as suggested by p62 accumulation (Figure 1d), due to the lysosomal disorder may occur. So, focusing on POMC-positive neurons, we studied dynamic changes of lysosomes by immunofluorescence microscopy, using antibodies against Lamp-2 and cathepsin B. Lamp-2 staining of the control POMC-positive neurons showed numerous tiny granules in the perinuclear region (Figure 4a), whereas coarse-granular immunoreactivities of Lamp-2 were seen after hydroxynonenal injections in the neurons which survived from hydroxynonenal toxicity (Figure 4b). Similarly, in the normal condition, cathepsin B immunoreactivity was visualized as a punctuate pattern of fluorescence, and was co-stained with Lamp-2, showing a merged color of yellow dots (Figure 5a). In the normal condition, both cathepsin B and Lamp-2 were thought to be confined within intact lysosomes. In contrast, after hydroxynonenal injections, cathepsin B immunofluorescence in POMC-positive neurons (Figure 5b rectangle) showed an enlarged staining double-positive for Lamp-2 in the arcuate nucleus (Figure 5b). Each of cathepsin B and Lamp-2 immunoreactivities showed a coarse-granular pattern with the merged color of yellow in the surviving POMC neurons after hydroxynonenal injections (Figure 5b). Enlarged immunoreactive area double-positive for cathepsin B and Lamp-2, indicated lysosomal membrane permeabilization.

In order to confirm the lysosomal membrane permeabilization, electron-microscopic analysis was done in the arcuate nucleus neurons, which are degenerating but still alive (Figure 1a circles). Showing a contrast to the membrane-bound lysosomes (Figures 3a arrows and 6a arrow head), many lysosomes showed distinct membrane permeabilization (Figures 6a stars and 6b). This was consistent with the findings of Lamp-2 and cathepsin B immunostainings (Figures 4b and 5b). Heat shock protein 70 (Hsp70) was reported to stabilize lysosomal membrane by binding to the endolysosomal lipid bis(monoacylglycero)phosphate (BMP) [57,58]. Simultaneously, the authors have reported implication of activated μ-calpain-mediated cleavage of the oxidized (carbonylated) Hsp70.1 as a cause of lysosomal membrane permeabilization/rupture [2,41,59,60], because Hsp70.1 has dual functions not only as a chaperone protein but also as a lysosomal stabilizer [57,58,61]. So, here we studied dynamic changes of activated μ-calpain and Hsp70.1 in the POMC neurons of the arcuate nucleus. After hydroxynonenal injections, immunoreactivities of both Hsp70.1 and activated μ-calpain were increased in the POMC-positive neurons of the arcuate nucleus (Figures 7b and 7f), compared to the control (Figures 7a and 7e). Interestingly the immunoreactivity of GPR40 was also remarkably increased along with Hsp70.1 in the POMC neurons after hydroxynonenal injections (Figure 7d), compared to the control (Figure 7c).

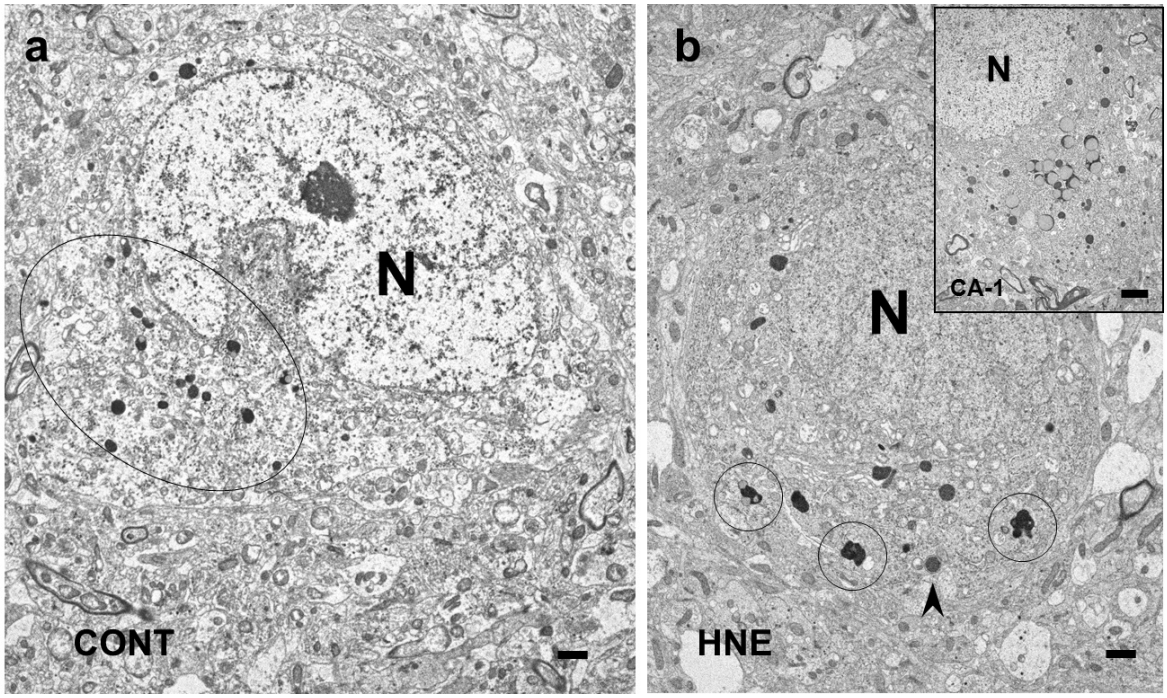

Figure 2: Electron-microphotographs of control (a) and degenerating (b) arcuate nucleus neurons before and after hydroxynonenal injections. a: Many lysosomes are distributed in the perinuclear cytoplasm (circle), but autophagosomes are scarcely seen in the control neuron (CONT). N: Nucleus, bar=1 μm b: After hydroxynonenal (HNE) injections, the normal lysosomes are decreased with very few remaining in the close vicinity of the nucleus. In contrast, autophagosomes are increased in the perinuclear soma (circles). An increment of autophagosomes was similarly observed in the hippocampal CA-1 neurons (rectangle) of the same monkey, which showed much stronger degeneration after hydroxynonenal injections. The degenerating neuron shows shrinkage of the cytoplasm being surrounded by enlarged dendritic processes, which is consistent with the microscopic finding (Figure 1a open arrows). N: Nucleus, bar=1 μm, (rectangle, bar=2 μm).

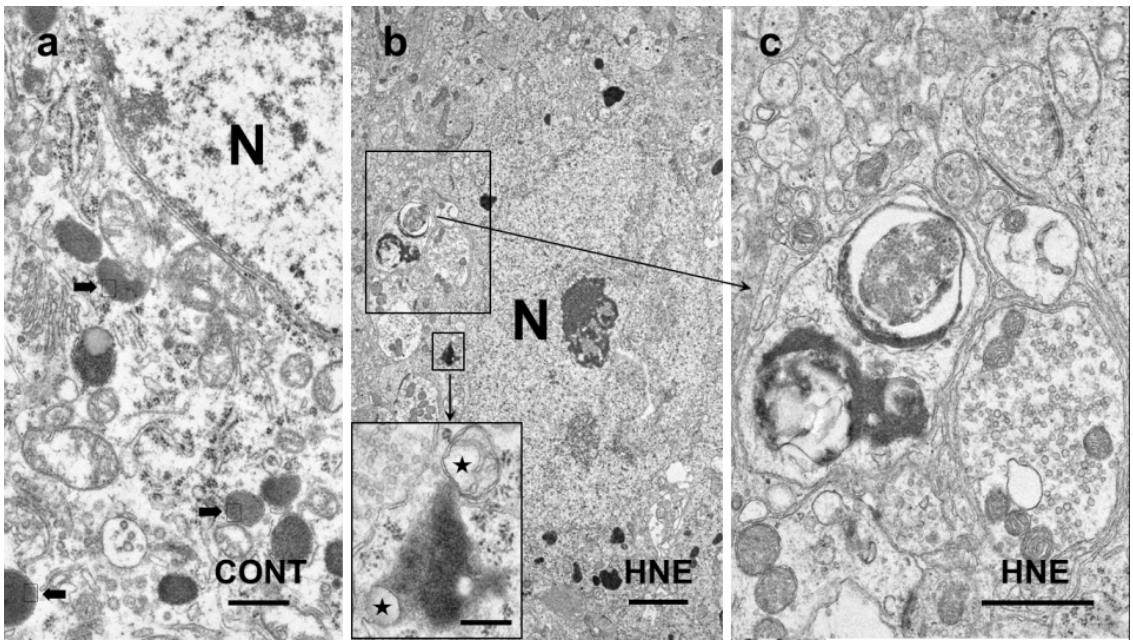

Figure 3: Electron-microphotographs of control (a) and degenerating (b,c) arcuate nucleus neurons before and after hydroxynonenal injections. a: In the control neuron (CONT), many lysosomes being bound by the distinct limiting membrane (arrows) are seen in the perinuclear soma. These lysosomes show distinct features from autophagosomes (b, middle and lower rectangles) in size, shape, and presence of the limiting membrane. N: Nucleus, bar=500 nm b: A magnified view of the middle rectangle shows an autophagosome with an irregular configuration and loss of the limiting membrane (lower rectangle). Damaged mitochondria-like structures (stars) are seen within and adjacent to the autophagosome (lower rectangle). N: Nucleus, HNE: Hydroxynonenal, bar=2 μm (rectangle, bar=500 nm) c: A magnified view of the upper rectangle in Figure 3b shows a remarkable degeneration of the dendritic processes. Dissolution of the synaptic vesicles and membranes form electron-dense, lamellar structures and aggregates of vesicles, which were never seen in the control (CONT) neurons. HNE: Hydroxynonenal, bar=1 μm.

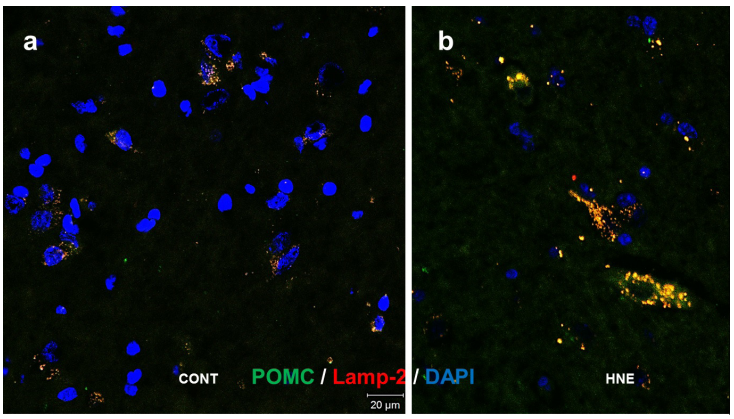

Figure 4: Immunofluorescence histochemical double-staining of POMC (green) and Lamp-2 (red). a: POMC-positive neurons of the control monkey show numerous, tiny yellow dots, showing Lamp-2-positive lysosomes. b: Merged color (yellow) of POMC and Lamp-2 is remarkably enlarged as coarse granules after hydroxynonenal (HNE) injections, which indicates lysosomal membrane permeabilization in the degenerating, but still alive, POMC neurons. DAPI-positive cell nuclei (blue) are remarkably decreased after hydroxynonenal injections, as shown in Figure 1c.

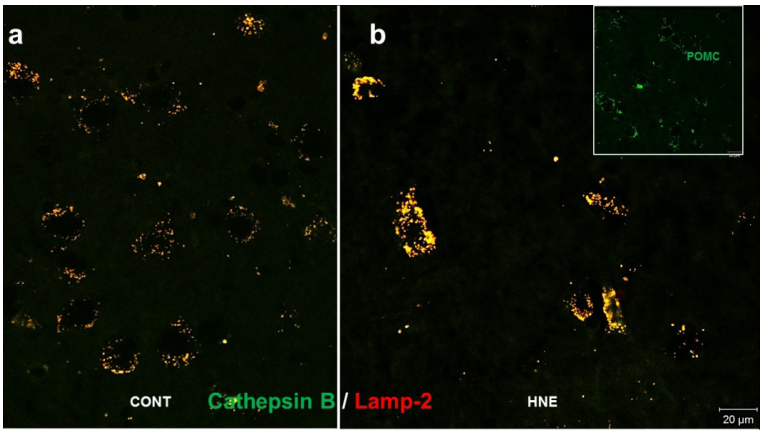

Figure 5: Immunofluorescence histochemical double-staining of cathepsin B (green) and Lamp-2 (red). a: POMC-positive neurons of the control (CONT) monkey shows tiny yellow dots, indicating cathepsin B- and Lamp-2-double-positive, normal lysosomes. b: Merged color (yellow) of cathepsin B and Lamp-2 is remarkably enlarged after hydroxynonenal (HNE) injections, which indicate lysosomal membrane permeabilization in the surviving neurons. Rectangle shows that these large, triangle cells were identified to be positive for POMC (rectangle).

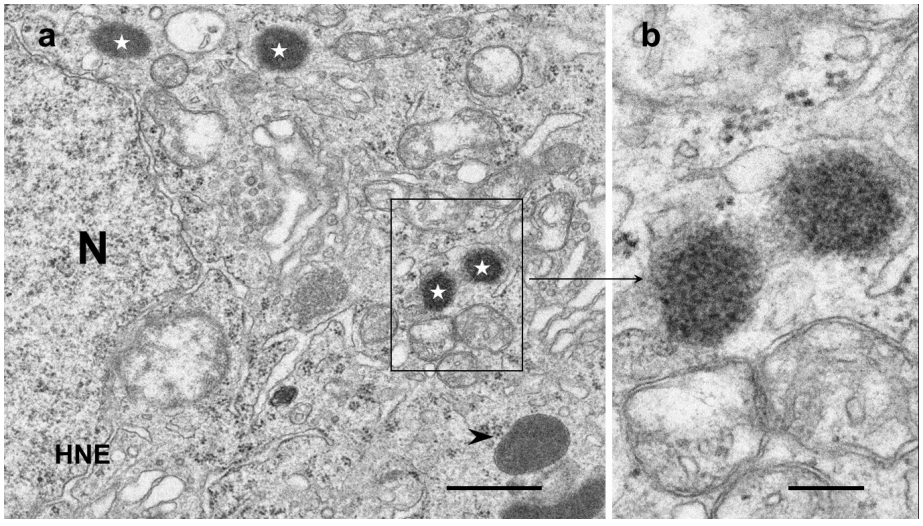

Figure 6: Electron-microphotographs of the degenerating neuron in the arcuate nucleus after hydroxynonenal (HNE) injections. a: Lysosomes with irregular contour (stars) exhibit evidence of the membrane destabilization, showing a marked contrast to the lysosome with distinct limiting membrane (arrow head). bar =1 μm. b: A magnified view of the Figure 6a rectangle shows evidence of lysosomal membrane destabilization with loss of the limiting membrane after hydroxynonenal injections. bar=200 nm.

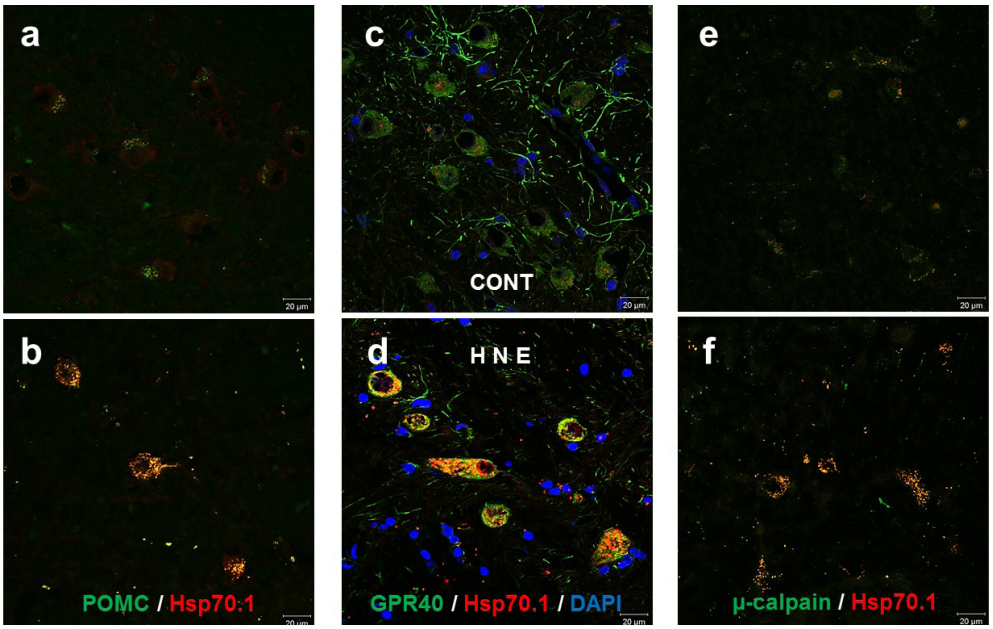

Figure 7: Immunofluorescence histochemical double-staining of POMC/Hsp70.1, GPR40/Hsp70.1, and activated μ-calpain/ Hsp70.1 (green/red, respectively) in the POMC neurons. a, b: Hsp70.1 immunoreactivity is increased in the POMC-positive neurons after hydroxynonenal (HNE) injections (b), compared to the control (CONT)(a). c, d: Merged color (yellow) of GPR40 and Hsp70.1 immunoreactivity is remarkably increased after hydroxynonenal injections (d), compared to the control (c). DAPI staining (blue). e, f: Merged color (yellow) of activated μ-calpain and Hsp70.1 immunoreactivity is negligible in the control neurons (e), but both were increased after hydroxynonenal injections and colocalized as a punctuate pattern (f). This indicates a possible interaction of activated μ-calpain upon Hsp70.1, i.e. activated μ-calpain-mediated cleavage of Hsp70.1.

Western blotting data of the arcuate nucleus were essentially consistent with the results of immunohistochemical analysis. However, due to both the essentially small number of POMC neurons in the arcuate nucleus and the remarkable neuronal loss after the consecutive injections of hydroxynonenal, the changes of band intensity were less remarkable on Western blotting, compared to the immunohistochemical analysis. Although a remarkable increase of p62 (Figure 1c), Hsp70.1 (Figure 7b), and μ-calpain (Figure 7f) immunoreactivity was observed within POMC neurons compared to the control (Figures 1c, 7a and 7e), the change of band intensities was less remarkable on Western blotting (Figure 8). This is presumably because change of the protein expression within the very small number of POMC neurons (Figure 1b) was hardly detected in the homogenized tissues. However, increased band intensities of GPR40 and activated μ-calpain were distinct after hydroxynonenal injections, compared to the control (Figure 8). There were only minor upregulations of main bands (70 kDa) and cleaved bands (~30 kDa) of Hsp70.1 and P62 bands (Figure 8).

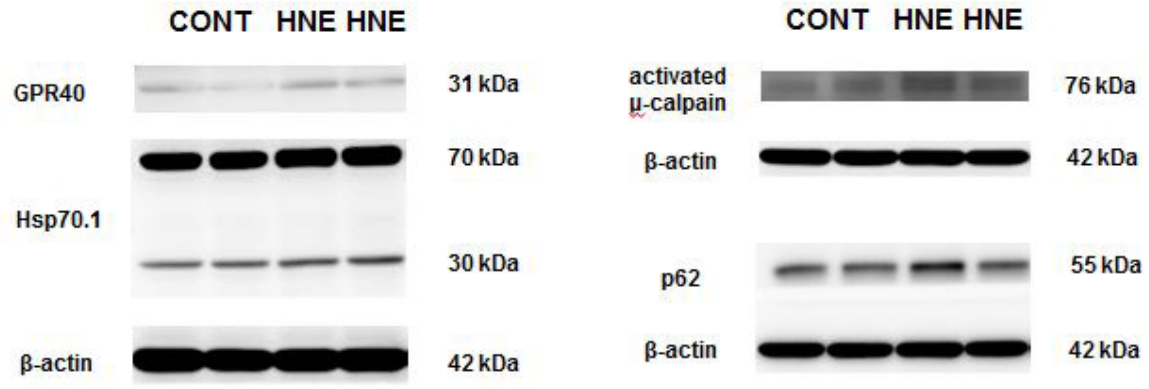

Figure 8: Western blotting analyses of GPR40, Hsp70.1, activated μ-calpain, and p62. Compared to the control (CONT), band intensities of GPR40 and activated μ-calpain are increased after hydroxynonenal (HNE) injections. Increments of cleaved Hsp70.1 band and p62 band intensities were less distinct, presumably due to the remarkable loss of POMC neurons after hydroxynonenal injections. However, because of the long-term stress due to hydroxynonenal, slight increments of Hsp70.1 main bands and their cleaved bands of ~30 kDa were confirmed after hydroxynonenal injections.

Discussion

Lysosomal membrane disintegrity

Soon after the discovery of lysosomes, in 1966 de Duve and Wattiaux formulated the "suicide bag hypothesis," which proposed that cell death is caused by the release of lysosomal hydrolases into the cytoplasm due to the lysosomal membrane destabilization [62,63]. Since a significant amount of intralysosomal acid phosphatases was observed to leak through ultrastructurally-intact lysosomal limiting membranes in the cultured glioma cells, the concept of 'lysosomal membrane permeabilization' was reported by Brunk and Ericsson in 1972 [64]. These pioneer researchers thought that lysosomal hydrolases may leak through the ultrastructurally-intact lysosomal membranes, but not through the ruptured sites at the limiting membrane. Therefore, for the long time lysosomes had been incorrectly considered sturdy organelles that do not disintegrate until the cell is already devitalized [65]. However, Yamashima et al. first reported ultrastructural evidence of 'lysosomal membrane rupture' in the degenerating, but still alive, hippocampal CA-1 neurons of the Japanese macaque monkeys after transient global brain ischemia [66]. Since their report, it became widely accepted that the 'lysosomal membrane rupture' causes programmed cell necrosis by the uncontrolled release of cathepsins [59,60,66-70].

For many years after de Duve's report, it has been believed that lysosomal cell death is unregulated and necrotic. The present study also showed evidence of necrosis (Figure 1a), but not apoptosis, in the POMC neurons of monkeys after hydroxynonenal injections. Since these POMC neurons showed a remarkable decrease of vivid lysosomes (Figures 2 and 3), it is reasonable to speculate that the 'lysosomal membrane rupture' had occurred during each hydroxynonenal injections, and most of the lysosomes disappeared until 12 weeks of the experiment. It is likely that the small number of surviving lysosomes at 12 weeks showed 'lysosomal membrane permeabilization', but more common feature during the consecutive hydroxynonenal injections was thought to be 'lysosomal membrane rupture'. Lysosomal membrane disintegrity which is induced by agents such as ROS, sphingosine, and free fatty acid, provokes extra-lysosomal release of cathepsins B, D, and L [2,33,71-74]. There is a strong correlation between the extent of free fatty acid accumulation and the severity of ischemic and traumatic injuries [75-77]. This is because the degradation of membrane phospholipids by activated intracellular phospholipases, causes high levels of free fatty acid and results in the cellular lipid overload [78,79]. Accordingly, lipotoxicity-mediated cell degeneration/death is currently emerging as an underlying factor contributing to diverse lifestyle-related diseases such as stroke, Alzheimer's disease, nonalcoholic liver diseases, and type 2 diabetes [51,80,81]. However, the molecular mechanism of lipotoxicity remains grossly unknown until now.

Ca^{2+}-activated papain-like protease, μ-calpain (EC 3.4.22.17) is well known to play physiological roles in cell division, movement, signal transduction, tissue repair, and remodeling programs [82-84]. Excessive calpain activation, however, plays a critical role in the progression of cell degeneration/death, because activated μ-calpain cleaves essential lysosomal membrane proteins such as Hsp70.1 and Lamp-2 which participate for the cell survival. By the cleavage of Hsp70.1, calpain can induce neuronal cell death by the lysosomal rupture [85]. Calpain-mediated cleavage of Lamp-2 also induces lysosomal membrane permeabilization after glucose deprivation in neuronal cells [86]. Therefore, excessive calpain activation is a common feature of diseases as cardiomyopathy, type 2 diabetes, ischemia/reperfusion injury, Alzheimer's disease, microbial infections, and cancers [2,59,60,66,69,81,87-89]. Although band intensities of activated μ-calpain were observed in this study both before and after hydroxynonenal injections on Western blot (Figure 8), it seems to be reasonable if considering role of calpain in both physiological and pathological conditions.

The present experimental paradigm showed that ω-6 PUFA-peroxidation product, hydroxynonenal, can induce μ-calpain activation in the POMC neurons (Figures 7e and 7f) and (Figure 8). As the rabbit anti-human activated μ-calpain antibody utilized in this study recognize only activated, but not inactivated, form of μ-calpain, its immunoreactivity co-localized with Hsp70.1 (Figure 7f) indicated interaction of activated μ-calpain upon Hsp70.1. Hsp70.1 is a stress-induced protein that confers cell protection against diverse stimuli by dual functions as a molecular chaperone and a lysosomal stabilizer. Accordingly, its dysfunction due to hydroxynonenal-mediated oxidation (carbonylation) followed by activated μ-calpain-mediated cleavage, induces neuronal degeneration/death *via* lysosomal membrane permeabilization/rupture, because the carbonylated Hsp70.1 [70] is vulnerable to activated μ-calpain [85]. Yamashima et al. recently reported that the calpain-cathepsin cascade is working not only in the ischemic (monkeys) and degenerative (humans) brains but also in the pancreas and liver (monkeys) after injections of the synthetic hydroxynonenal [2,51,52,60,70]. Since hydroxynonenal can induce μ-calpain activation and Hsp70.1 carbonylation simultaneously, it is reasonable to speculate that the calpain-cathepsin cascade is working in POMC neurons in response to hydroxynonenal (Figure 9). However, compared to the hippocampal CA-1, liver, and pancreas tissues with dense distribution of cells, demonstrating up-regulation of the calpain-mediated cleavage of carbonylated Hsp70.1 by the Western blotting was difficult in the arcuate nucleus with sparse distribution of POMC neurons especially after hydroxynonenal injections (Figure 1).

Autophagy deficiency

The present study showed evidence of autophagy deficiency such as accumulation of p62 (Figure 1d) and autophagosomes (Figures 2 and 3) within the degenerating POMC neuron of monkeys after hydroxynonenal injections. Autophagy is an important catabolic process for maintaining human health, as it prevents various diseases including neurodegenerative diseases, diabetes, and cancers [90-93]. For instance, age-related risks for Alzheimer's and Parkinson's diseases may be largely due to decreased neuronal capacity of degrading toxic proteins. Baseline (constitutive) autophagy occurs under physiological conditions, but it is increased by stress, starvation, or pathological conditions. During autophagy, autophagosomes engulf unwanted cytoplasmic content such as damaged organelles and macromolecules. Autophagosomes then fuse with lysosomes to form autolysosomes or autophagolysosomes [94,95], where the cargo components are degraded by lysosomal acid hydrolases such as cathepsins into amino acids, fatty acids, carbohydrolates, and nucleotides. Then, they are shuttled to the cytosol for the re-use in the cellular function [96]. Neurons are post-mitotic cells, with no ability to dilute damaged/aged proteins and organelles by cell division which is a strategy for survival commonly employed by mitotic cells. So, the long-term maintenance of neuronal health requires continuous removal of aggregated proteins and damaged/aged organelles *via* effective autophagy. The latter is particularly important for neurons, most of which last the lifetime of the organism. It maintains neuronal homeostasis by sequestering cytosolic cargo into autophagosomes and delivering it into lysosomes for degradation [97]. Accordingly, the lysosomal dysfunction in neurons leads to accumulation of undegraded autophagosomes, autophagy deficiency, which gives rise to blockade of the final autophagy pathway.

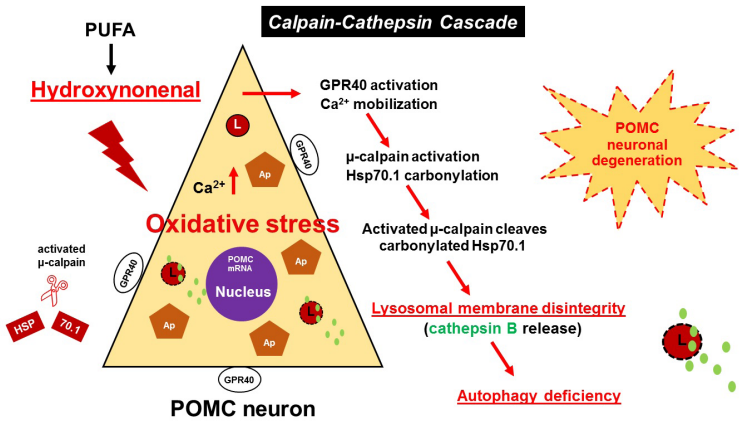

Figure 9: Flow chart of hydroxynonenal-induced lysosomal and autophagy disorder *via* the calpain-cathepsin cascade in POMC neurons. L (white): Normal lysosome; L (black): Lysosome with permeabilization of the limiting membrane; Ap: autophagosomes; Green dots: Cathepsin enzymes; PUFA: polyunsaturated fatty acid.

Autophagy in hypothalamic POMC neurons plays an important role in the control of appetite or body weight and the corresponding signaling [98]. As autophagy contributes to the quality control process for organelles, defects in hypothalamic autophagy lead to metabolic dysregulation. For instance, mice with specific deletion of autophagy-related 7 (Atg7), an essential autophagy gene, in hypothalamic POMC neurons, showed increased body weight, food intake, adiposity, decreased energy expenditure, leptin resistance, and glucose intolerance [15,98-100]. In addition, in the mice POMC neurons after the high-fat diet feeding, Thaler et al. found accumulation of autophagosomes engulfing damaged mitochondria as an evidence of autophagy failure. Intriguingly, these responses were shown to occur selectively in the POMC neurons not only of rodents but also of humans [42]. Interestingly, μ-calpain overactivation can block autophagy through cleavage of Beclin 1 (ATG6) and ATG5 [101-104]. Bechlin 1 is an autophagy inducer, while ATG5 is necessary not only for the formation of autophagosomes but also for the autophagosome-lysosome fusion [105,106]. Under excessive calpain-activated conditions due to the intensive stress, however, cleavage of Beclin 1 and ATG5 compromises autophagosome accumulation and autophagosome-lysosome fusion with the resultant autophagy failure [104,107,108]. P62, a specific substrate of autophagy, is also involved in diverse intracellular signal transduction systems [98,109,110]. It is suggested from accumulation of p62 and autophagosomes as shown here in the degenerating POMC neurons that hydroxynonenal induced not only lysosomal disorder but also autophagy deficiency by the activation of μ-calpain (Figure 9).

Mitochondrial ROS was reported to be important, basal, adaptive signaling molecules that indicate positive or negative energy states at the level of POMC and NPY/AgRP neurons in hypothalamus [111]. Fluctuating hypothalamic ROS levels direct food intake, energy expenditure, and glucose utilization [111]. When systemic glucose levels are physiologically high after an appropriate diet, blood glucose is taken up and oxidized by POMC neurons, leading to the generation of ATP and appropriate amount of ROS. When cellular ROS level reaches a threshold, they activate POMC neurons, enabling the cessation of feeding and initiation of storage in the form of fat or glycogen *via* processes controlled by insulin and leptin [11,112]. At the same time, elevating ROS in the hypothalamus may reduce activity of NPY/AgRP neurons that propagates hunger [113]. Upon exposure to high-fat diets and/or deep-fried foods, however, ROS levels increase excessively, which results not only in impaired satiety signaling in POMC neurons [111] but also in the occurrence of excessive Ca^{2+} mobilization and μ-calpain activation with the resultant POMC neuronal degeneration/death [2]. Cathepsins leaked from partially ruptured lysosomes cause downstream mitochondrial membrane permeabilization and stimulate generation of more ROS, which in turn triggers further lysosomal damage [48,114]. Oxidative stress and free radical damage play a principal role in cell death induced by lysosome dysfunction [115]. Both should be linked to alterations in the autophagy degradation pathway and lysosome membrane integrity [115-117].

As lysosomes are final executors of the autophagy pathway, the lysosomal disorder conceivably facilitates autophagy deficiency. Autophagy deficiency and lysosomal disintegrity in anorexigenic POMC neurons, may be a cause of failure in reducing food intake and increasing energy expenditure to induce obesity. Anti-ROS and/or hydroxynonenal detoxification therapies that protect lysosomal structure and restore autophagy function of POMC neurons would be required to treat hypothalamic resistance. Hydroxynonenal is known to increase in the serum with ageing, and to facilitate diverse lifestyle-related diseases. Although very difficult to demonstrate in humans, it should be elucidated whether cooking oil-derived hydroxynonenal causes lysosomal disorder and autophagy deficiency in POMC neurons.

Conclusion

In the Western diet there is an extremely high ω-6/ω-3 PUFA ratio, mostly because of high intake of deep-fried foods and low intake of fish. ω-6 PUFAs in vegetable oils and biomembranes are vulnerable to the oxidative stress such as deep-frying and environmental pollution, which generate exogenous or intrinsic hydroxynonenal. Here, the monkey experimental paradigm showed that lipid-peroxidation product hydroxynonenal induces activation of μ-calpain and upregulation of GPR40 in POMC neurons. In addition, hydroxynonenal induces lysosomal membrane disintegrity to cause leakage of intralysosomal cathepsins into the cytoplasm. Since Hsp70.1 has dual functions as lysosomal stabilizer and chaperone protein, the calpain-mediated cleavage of oxidized (carbonylated) Hsp70.1 conceivably contributed also to the occurrence of autophagy deficiency. Lysosomal disintegrity and autophagy deficiency, combined together, cause POMC neurodegeneration and loss of POMC neurons.

Conflict of Interest

The authors declare that they have no conflict of interest.

Financial Support

This work was supported by a grant (TeY) from Kiban-Kenkyu (B) (19H04029) from the Japanese Ministry of Education, Culture, Sports, Science and Technology.

References

1. Timper K, Brüning JC (2017) Hypothalamic circuits regulating appetite and energy homeostasis: Pathways to obesity. Dis Model Mech 10: 679-689.
2. Yamashima T, Ota T, Mizukoshi E, Nakamura H, Yamamoto Y, et al. (2020) Intake of ω-6 polyunsaturated fatty acid-rich vegetable oils and risk of lifestyle diseases. Adv Nutr 11:1489-1509.
3. Rodríguez EM, Blázquez JL, Guerra M (2010) The design of barriers in the hypothalamus allows the median eminence and the arcuate nucleus to enjoy private milieus: The former opens to the portal blood and the latter to the cerebrospinal fluid. Peptides 31: 757-776.
4. Cowley MA, Smart JL, Rubinstein M, Cerdán MG, Diano S, et al. (2001) Leptin activates anorexigenic POMC neurons through a neural network in the arcuate nucleus. Nature 411: 480-484.
5. Hill JW, Williams KW, Ye C, Luo J, Balthasar N, et al. (2008) Acute effects of leptin require PI3K signaling in hypothalamic proopiomelanocortin neurons in mice. J Clin Invest 118: 1796-1805.
6. van den Top M, Lee K, Whyment AD, Blanks AM, Spanswick D (2004) Orexigen-sensitive NPY/AgRP pacemaker neurons in the hypothalamic arcuate nucleus. Nat Neurosci 7:493-494.
7. Williams KW, Margatho LO, Lee CE, Choi M, Lee S, et al. (2010) Segregation of acute leptin and insulin effects in distinct populations of arcuate proopiomelanocortin neurons. J Neurosci 30:2472-2479.
8. Cowley MA, Smith RG, Diano S, Tschöp M, Pronchuk N, et al. (2003) The distribution and mechanism of action of ghrelin in the CNS demonstrates a novel hypothalamic circuit regulating energy homeostasis. Neuron 37: 649-661.
9. van den Pol AN, Yao Y, Fu L-Y, Foo K, Huang H, et al. (2009) Neuromedin B and gastrin-releasing peptide excite arcuate nucleus neuropeptide Y neurons in a novel transgenic mouse expressing strong Renilla green fluorescent protein in NPY neurons. J Neurosci 29: 4622-4639.
10. Yang Y, Atasoy D, Su HH, Sternson SM (2011) Hunger states switch a flip-flop memory circuit *via* a synaptic AMPK-dependent positive feedback loop. Cell 146: 992-1003.
11. Diano S (2011) New aspects of melanocortin signaling: A role for PRCP in α-MSH degradation. Front Neuroendocrinol 32: 70-83.
12. Koch M, Varela L, Kim JG, Kim JD, Hernández-Nuño F, et al. (2015) Hypothalamic POMC neurons promote cannabinoid-induced feeding. Nature 519: 45-50.
13. McClellan KM, Calver AR, Tobet SA (2008) GABAB receptors role in cell migration and positioning within the ventromedial nucleus of the hypothalamus. Neuroscience 151: 1119-1131.
14. Sternson SM, Atasoy D, Betley JN, Henry FE, Xu S (2016) An emerging technology framework for the neurobiology of appetite. Cell Metab 23: 234-253.
15. Toda C, Santoro A, Kim JD, Diano S (2017) POMC neurons: From birth to death. Annu Rev Physiol 79: 209-236.
16. Acuna-Goycolea C, van den Pol AN (2005) Peptide YY(3-36) inhibits both anorexigenic proopiomelanocortin and orexigenic neuropeptide Y neurons: implications for hypothalamic regulation of energy homeostasis. J Neurosci 25: 10510-10519.
17. Flier JS (2004) Obesity wars: Molecular progress confronts an expanding epidemic. Cell 116: 337-350.
18. Jo Y-H, Su Y, Gutierrez-Juarez R, Chua SJ (2009) Oleic acid directly regulates POMC neuron excitability in the hypothalamus. J Neurophysiol 101: 2305-2316.
19. Schwartz MW, Porte DJ (2005) Diabetes, obesity, and the brain. Science 307: 375-379.
20. Schwartz MW, Woods SC, Porte DJ, Seeley RJ, Baskin DG (2000) Central nervous system control of food intake. Nature 404: 661-671.
21. Spanswick D, Smith MA, Groppi VE, Logan SD, Ashford ML (1997) Leptin inhibits hypothalamic neurons by activation of ATP-sensitive potassium channels. Nature 390: 521-525.
22. Spanswick D, Smith MA, Mirshamsi S, Routh VH, Ashford ML (2000) Insulin activates ATP-sensitive K^+ channels in hypothalamic neurons of lean, but not obese rats. Nat Neurosci 3: 757-758.
23. Wang R, Liu X, Hentges ST, Dunn-Meynell AA, Levin BE, et al. (2004) The regulation of glucose-excited neurons in the hypothalamic arcuate nucleus by glucose and feeding-relevant peptides. Diabetes 53: 1959-1965.
24. Mountjoy KG, Wong J (1997) Obesity, diabetes and functions for proopiomelanocortin-derived peptides. Mol Cell Endocrinol 128: 171-177.
25. Lam TKT, Pocai A, Gutierrez-Juarez R, Obici S, Bryan J, et al. (2005) Hypothalamic sensing of circulating fatty acids is required for glucose homeostasis. Nat Med 11: 320-327.
26. Lam TKT, Schwartz GJ, Rossetti L (2005) Hypothalamic sensing of fatty acids. Nat Neurosci 8: 579-584.
27. Kaushik S, Arias E, Kwon H, Lopez NM, Athonvarangkul D, et al. (2012) Loss of autophagy in hypothalamic POMC neurons impairs lipolysis. EMBO Rep 13: 258-265.
28. Könner AC, Brüning JC (2012) Selective insulin and leptin resistance in metabolic disorders. Cell Metab 16: 144-152.
29. Martínez de Morentin PB, Varela L, Fernø J, Nogueiras R, Diéguez C, et al. (2010) Hypothalamic lipotoxicity and the metabolic syndrome. Biochim Biophys Acta 1801: 350-361.
30. Ozcan L, Ergin AS, Lu A, Chung J, Sarkar S, et al. (2009) Endoplasmic reticulum stress plays a central role in development of leptin resistance. Cell Metab 9: 35-51.
31. Velloso LA, Schwartz MW (2011) Altered hypothalamic function in diet-induced obesity. Int J Obes (Lond) 35: 1455-1465.
32. Waise TMZ, Toshinai K, Naznin F, NamKoong C, Md Moin AS, et al. (2015) One-day high-fat diet induces inflammation in the nodose ganglion and hypothalamus of mice. Biochem Biophys Res Commun 464: 1157-1162.
33. Briscoe CP, Tadayyon M, Andrews JL, Benson WG, Chambers JK, et al. (2003) The orphan G protein-coupled receptor GPR40 is activated by medium and long chain fatty acids. J Biol Chem 278: 11303-11311.
34. Itoh Y, Kawamata Y, Harada M, Kobayashi M, Fujii R, et al. (2003) Free fatty acids regulate insulin secretion from pancreatic beta cells through GPR40. Nature 422: 173-176.
35. Boneva NB, Yamashima T (2012) New insights into "GPR40-CREB interaction in adult neurogenesis" specific for primates. Hippocampus 22: 896-905.
36. Khan MZ, He L (2017) The role of polyunsaturated fatty acids and GPR40 receptor in brain. Neuropharmacology 113: 639-651.
37. Ma D, Tao B, Warashina S, Kotani S, Lu L, et al. (2007) Expression of free fatty acid receptor GPR40 in the central nervous system of adult monkeys. Neurosci Res 58: 394-401.
38. Yamashima T (2012) "PUFA-GPR40-CREB signaling" hypothesis for the adult primate neurogenesis. Prog Lipid Res 51: 221-231.
39. Yamashima T (2015) Dual effects of the non-esterified fatty acid receptor "GPR40" for human health. Prog Lipid Res 58: 40-50.
40. Moraes JC, Coope A, Morari J, Cintra DE, Roman EA, et al. (2009) High-fat diet induces apoptosis of hypothalamic neurons. PLoS One 4: e5045.
41. van de Sande-Lee S, Pereira FRS, Cintra DE, Fernandes PT, Cardoso AR, et al. (2011) Partial reversibility of hypothalamic dysfunction and changes in brain activity after body mass reduction in obese subjects. Diabetes 60: 1699-1704.
42. Thaler JP, Yi C-X, Schur EA, Guyenet SJ, Hwang BH, et al. (2012) Obesity is associated with hypothalamic injury in rodents and humans. J Clin Invest 122: 153-162.
43. Mancini AD, Poitout V (2013) The fatty acid receptor FFA1/GPR40 a decade later: How much do we know? Trends Endocrinol Metab 24: 398-407.
44. Honoré J-C, Kooli A, Hamel D, Alquier T, Rivera J-C, et al. (2013) Fatty acid receptor Gpr40 mediates neuromicrovascular degeneration induced by transarachidonic acids in rodents. Arterioscler Thromb Vasc Biol 33: 954-961.
45. Kermorvant-Duchemin E, Sennlaub F, Sirinyan M, Brault S, Andelfinger G, et al. (2005) Trans-arachidonic acids generated during nitrative stress induce a thrombospondin-1-dependent microvascular degeneration. Nat Med 11: 1339-1345.

46. Park S, Jang A, Bouret SG (2020) Maternal obesity-induced endoplasmic reticulum stress causes metabolic alterations and abnormal hypothalamic development in the offspring. PLoS Biol 18: e3000296.

47. Posey KA, Clegg DJ, Printz RL, Byun J, Morton GJ, et al. (2009) Hypothalamic proinflammatory lipid accumulation, inflammation, and insulin resistance in rats fed a high-fat diet. Am J Physiol Endocrinol Metab 296: E1003-12.

48. Li Z, Berk M, McIntyre TM, Gores GJ, Feldstein AE (2008) The lysosomal-mitochondrial axis in free fatty acid-induced hepatic lipotoxicity. Hepatology 47: 1495-1503.

49. Ramalingam M, Kim S-J (2012) Reactive oxygen/nitrogen species and their functional correlations in neurodegenerative diseases. J Neural Transm 119: 891-910.

50. Simopoulos AP (2008) The importance of the omega-6/omega-3 fatty acid ratio in cardiovascular disease and other chronic diseases. Exp Biol Med (Maywood) 233: 674-688.

51. Boontem P, Yamashima T (2021) Hydroxynonenal causes Langerhans cell degeneration in the pancreas of Japanese macaque monkeys. PLoS One 16: e0245702.

52. Yamashima T (2021) Hydroxynonenal makes Alzheimer pathology without amyloid β: Which is a real culprit? J Alzheimers Dis Park 11.

53. Schaur RJ, Siems W, Bresgen N, Eckl PM (2015) 4-Hydroxy-nonenal-A bioactive lipid peroxidation product. Biomolecules 5: 2247-2337.

54. Bjørkøy G, Lamark T, Brech A, Outzen H, Perander M, et al. (2005) p62/SQSTM1 forms protein aggregates degraded by autophagy and has a protective effect on huntingtin-induced cell death. J Cell Biol 171: 603-614.

55. Komatsu M, Waguri S, Koike M, Sou Y-S, Ueno T, et al. (2007) Homeostatic levels of p62 control cytoplasmic inclusion body formation in autophagy-deficient mice. Cell 131: 1149-1163.

56. Sergin I, Razani B (2014) Self-eating in the plaque: What macrophage autophagy reveals about atherosclerosis. Trends Endocrinol Metab 25: 225-234.

57. Kirkegaard T, Jäättelä M (2009) Lysosomal involvement in cell death and cancer. Biochim Biophys Acta 1793: 746-754.

58. Kirkegaard T, Roth AG, Petersen NHT, Mahalka AK, Olsen OD, et al. (2010) Hsp70 stabilizes lysosomes and reverts Niemann-Pick disease-associated lysosomal pathology. Nature 463: 549-553.

59. Yamashima T (2013) Reconsider Alzheimer's disease by the 'calpain-cathepsin hypothesis'--a perspective review. Prog Neurobiol 105: 1-23.

60. Yamashima T (2016) Can "calpain-cathepsin hypothesis" explain Alzheimer neuronal death? Ageing Res Rev 32: 169-179.

61. Balogi Z, Multhoff G, Jensen TK, Lloyd-Evans E, Yamashima T, et al. (2019) Hsp70 interactions with membrane lipids regulate cellular functions in health and disease. Prog Lipid Res 74: 18-30.

62. De Duve C, Wattiaux R (1966) Functions of lysosomes. Annu Rev Physiol 28: 435-492.

63. Lüllmann-Rauch R (2005) History and morphology of the lysosome. In: Saftig P (ed) Lysosomes. Springer US, Boston, MA.

64. Brunk UT, Ericsson JL (1972) Cytochemical evidence for the leakage of acid phosphatase through ultrastructurally intact lysosomal membranes. Histochem J 4: 479-491.

65. Terman A, Kurz T, Gustafsson B, Brunk UT (2006) Lysosomal labilization. IUBMB Life 58: 531-539.

66. Yamashima T, Saido TC, Takita M, Miyazawa A, Yamano J, et al. (1996) Transient brain ischaemia provokes Ca^{2+}, PIP_2 and calpain responses prior to delayed neuronal death in monkeys. Eur J Neurosci 8: 1932-1944.

67. Oikawa S, Yamada T, Minohata T, Kobayashi H, Furukawa A, et al. (2009) Proteomic identification of carbonylated proteins in the monkey hippocampus after ischemia-reperfusion. Free Radic Biol Med 46: 1472-1477.

68. Yamashima T (2000) Implication of cysteine proteases calpain, cathepsin and caspase in ischemic neuronal death of primates. Prog Neurobiol 62: 273-295.

69. Yamashima T, Kohda Y, Tsuchiya K, Ueno T, Yamashita J, et al. (1998) Inhibition of ischaemic hippocampal neuronal death in primates with cathepsin B inhibitor CA-074: A novel strategy for neuroprotection based on "calpain-cathepsin hypothesis". Eur J Neurosci 10: 1723-1733.

70. Yamashima T, Oikawa S (2009) The role of lysosomal rupture in neuronal death. Prog Neurobiol 89: 343-358.

71. Boya P, Andreau K, Poncet D, Zamzami N, Perfettini J-L, et al. (2003) Lysosomal membrane permeabilization induces cell death in a mitochondrion-dependent fashion. J Exp Med 197: 1323-1334.

72. Hook V, Yoon M, Mosier C, Ito G, Podvin S, et al. (2020) Cathepsin B in neurodegeneration of Alzheimer's disease, traumatic brain injury, and related brain disorders. Biochim Biophys acta Proteins proteomics 1868: 140428.

73. Lie PPY, Nixon RA (2019) Lysosome trafficking and signaling in health and neurodegenerative diseases. Neurobiol Dis 122: 94-105.

74. Liu X-J, Yang W, Qi J-S (2012) [Oxidative stress and Alzheimer's disease]. Sheng Li Xue Bao 64: 87-95.

75. Bazan NGJ, de Bazan HE, Kennedy WG, Joel CD (1971) Regional distribution and rate of production of free fatty acids in rat brain. J Neurochem 18: 1387-1393.

76. Dhillon HS, Carman HM, Zhang D, Scheff SW, Prasad MR (1999) Severity of experimental brain injury on lactate and free fatty acid accumulation and Evans blue extravasation in the rat cortex and hippocampus. J Neurotrauma 16: 455-469.

77. Zhang JP, Sun GY (1995) Free fatty acids, neutral glycerides, and phosphoglycerides in transient focal cerebral ischemia. J Neurochem 64: 1688-1695.

78. Farooqui AA, Horrocks LA (1998) Lipid peroxides in the free radical pathophysiology of brain diseases. Cell Mol Neurobiol 18: 599-608.

79. Farooqui AA, Horrocks LA (2006) Phospholipase A2-generated lipid mediators in the brain: The good, the bad, and the ugly. Neurosci 12: 245-260.

80. Almaguel FG, Liu J-W, Pacheco FJ, Casiano CA, De Leon M (2009) Activation and reversal of lipotoxicity in PC12 and rat cortical cells following exposure to palmitic acid. J Neurosci Res 87: 1207-1218.

81. Shimabukuro M, Zhou YT, Levi M, Unger RH (1998) Fatty acid-induced beta cell apoptosis: A link between obesity and diabetes. Proc Natl Acad Sci U S A 95: 2498-2502.

82. Murachi T (1983) Calpain and calpastatin. Trends Biochem Sci 8: 167-169.

83. Sorimachi H, Ishiura S, Suzuki K (1997) Structure and physiological function of calpains. Biochem J 328: 721-732.

84. Suzuki K, Hata S, Kawabata Y, Sorimachi H (2004) Structure, activation, and biology of calpain. Diabetes 53: S8-12.

85. Sahara S, Yamashima T (2010) Calpain-mediated Hsp70.1 cleavage in hippocampal CA1 neuronal death. Biochem Biophys Res Commun 393: 806-811.

86. Gerónimo-Olvera C, Montiel T, Rincon-Heredia R, Castro-Obregón S, Massieu L (2017) Autophagy fails to prevent glucose deprivation/glucose reintroduction-induced neuronal death due to calpain-mediated lysosomal dysfunction in cortical neurons. Cell Death Dis 8: e2911.

87. Chakraborti S, Alam MN, Paik D, Shaikh S, Chakraborti T (2012) Implications of calpains in health and diseases. Indian J Biochem Biophys 49: 316-328.

88. Storr SJ, Carragher NO, Frame MC, Parr T, Martin SG (2011) The calpain system and cancer. Nat Rev Cancer 11: 364-374.

89. Zatz M, Starling A (2005) Calpains and disease. N Engl J Med 352: 2413-2423.

90. Kroemer G, Levine B (2008) Autophagic cell death: The story of a misnomer. Nat Rev Mol Cell Biol 9: 1004-1010.

91. Levine B, Kroemer G (2008) Autophagy in the pathogenesis of disease. Cell 132: 27-42.

92. Mizushima N, Levine B, Cuervo AM, Klionsky DJ (2008) Autophagy fights disease through cellular self-digestion. Nature 451: 1069-1075.

93. Yim WW-Y, Mizushima N (2020) Lysosome biology in autophagy. Cell Discov 6: 6.

94. Maday S, Holzbaur ELF (2014) Autophagosome biogenesis in primary neurons follows an ordered and spatially regulated pathway. Dev Cell 30: 71-85.

95. Maday S, Wallace KE, Holzbaur ELF (2012) Autophagosomes initiate distally and mature during transport toward the cell soma in primary neurons. J Cell Biol 196: 407-417.

96. Levine B, Klionsky DJ (2004) Development by self-digestion: Molecular mechanisms and biological functions of autophagy. Dev Cell 6:463-477.

97. Singh R, Cuervo AM (2011) Autophagy in the cellular energetic balance. Cell Metab 13: 495-504.

98. Quan W, Kim H-K, Moon E-Y, Kim SS, Choi CS, et al. (2012) Role of hypothalamic proopiomelanocortin neuron autophagy in the control of appetite and leptin response. Endocrinology 153: 1817-1826.

99. Coupé B, Ishii Y, Dietrich MO, Komatsu M, Horvath TL, et al. (2012) Loss of autophagy in pro-opiomelanocortin neurons perturbs axon growth and causes metabolic dysregulation. Cell Metab 15: 247-255.

100. Meng Q, Cai D (2011) Defective hypothalamic autophagy directs the central pathogenesis of obesity *via* the IkappaB kinase beta (IKKbeta)/NF-kappaB pathway. J Biol Chem 286: 32324-32332.

101. Lépine S, Allegood JC, Edmonds Y, Milstien S, Spiegel S (2011) Autophagy induced by deficiency of sphingosine-1-phosphate phosphohydrolase 1 is switched to apoptosis by calpain-mediated autophagy-related gene 5 (Atg5) cleavage. J Biol Chem 286: 44380-44390.

102. Russo R, Berliocchi L, Adornetto A, Varano GP, Cavaliere F, et al. (2011) Calpain-mediated cleavage of Beclin-1 and autophagy deregulation following retinal ischemic injury *in vivo*. Cell Death Dis 2: e144.

103. Shi M, Zhang T, Sun L, Luo Y, Liu D-H, et al. (2013) Calpain, Atg5 and Bak play important roles in the crosstalk between apoptosis and autophagy induced by influx of extracellular calcium. Apoptosis 18: 435-451.

104. Yousefi S, Perozzo R, Schmid I, Ziemiecki A, Schaffner T, et al. (2006) Calpain-mediated cleavage of Atg5 switches autophagy to apoptosis. Nat Cell Biol 8: 1124-1132.

105. Chen D, Fan W, Lu Y, Ding X, Chen S, et al. (2012) A mammalian autophagosome maturation mechanism mediated by TECPR1 and the Atg12-Atg5 conjugate. Mol Cell 45: 629-641.

106. Ye X, Zhou X-J, Zhang H (2018) Exploring the role of autophagy-related gene 5 (ATG5) yields important insights into autophagy in autoimmune/autoinflammatory diseases. Front Immunol 9: 2334.

107. Xia H-G, Zhang L, Chen G, Zhang T, Liu J, et al. (2010) Control of basal autophagy by calpain1 mediated cleavage of ATG5. Autophagy 6: 61-66.

108. Zhu X, Messer JS, Wang Y, Lin F, Cham CM, et al. (2015) Cytosolic HMGB1 controls the cellular autophagy/apoptosis checkpoint during inflammation. J Clin Invest 125: 1098-1110.

109. Kim JY, Ozato K (2009) The sequestosome 1/p62 attenuates cytokine gene expression in activated macrophages by inhibiting IFN regulatory factor 8 and TNF receptor-associated factor 6/NF-kappaB activity. J Immunol 182: 2131-2140.

110. Moscat J, Diaz-Meco MT, Wooten MW (2007) Signal integration and diversification through the p62 scaffold protein. Trends Biochem Sci 32: 95-100.

111. Shadel GS, Horvath TL (2015) Mitochondrial ROS signaling in organismal homeostasis. Cell 163: 560-569.

112. Varela L, Horvath TL (2012) AgRP neurons: A switch between peripheral carbohydrate and lipid utilization. EMBO J 31: 4252-4254.

113. Andrews ZB, Liu Z-W, Walllingford N, Erion DM, Borok E, et al. (2008) UCP2 mediates ghrelin's action on NPY/AgRP neurons by lowering free radicals. Nature 454: 846-851.

114. Ghavami S, Asoodeh A, Klonisch T, Halayko AJ, Kadkhoda K, et al. (2008) Brevinin-2R(1) semi-selectively kills cancer cells by a distinct mechanism, which involves the lysosomal-mitochondrial death pathway. J Cell Mol Med 12: 1005-1022.

115. Pivtoraiko VN, Stone SL, Roth KA, Shacka JJ (2009) Oxidative stress and autophagy in the regulation of lysosome-dependent neuron death. Antioxid Redox Signal 11: 481-496.

116. Gutiérrez IL, González-Prieto M, García-Bueno B, Caso JR, Leza JC, et al. (2018) Alternative method to detect neuronal degeneration and amyloid β accumulation in free-floating brain sections with fluoro-jade. ASN Neuro 10: 1759091418784357.

117. Schmued LC, Stowers CC, Scallet AC, Xu L (2005) Fluoro-Jade C results in ultra high resolution and contrast labeling of degenerating neurons. Brain Res 1035: 24-31.